eprints@whiterose.ac.uk
https://eprints.whiterose.ac.uk/

Low sintering temperature, temperature-stable scheelite structured Bi[V$_{1-x}$ (Fe$_{1/3}$W $_{2/3}$)$_x$]O$_4$ microwave dielectric ceramics

Fang-Fang Wu,[a] Di Zhou,*[a] Song Xia,[a] Ling Zhang,[a] Feng Qiao,[a] Li-Xia Pang,[b] Shi-Kuan Sun,[c] Tao Zhou,[d] Charanjeet Singh,[e] Antonio Sergio Bezerra Sombra,[f] Moustafa Adel Darwish,[g] Ian M. Reaney [h]

[a]Key Laboratory of Multifunctional Materials and Structures, Ministry of Education, School of Electronic Science and Engineering, Xi'an Jiaotong University, Xi'an 710049, Shaanxi, China

[b]Micro-optoelectronic Systems Laboratories, Xi'an Technological University, Xi'an, Shaanxi 710032, China

[c]School of Material Science and Energy Engineering, Foshan University, Foshan, Guangdong, 528000, China

[d]School of Electronic and Information Engineering, Hangzhou Dianzi University, Hangzhou, 310018, China

[e]School of Electronics and Communication Engineering, Lovely Professional University, Jalandhar, Punjab, India

[f]Telecommunication Engineering Department, Federal University of Ceará (UFC), Fortaleza, Ceará 60755-640, Brazil; Telecommunication and Materials Science and Engineering of Laboratory (LOCEM), Physics Department, Federal University of Ceará (UFC), Pici Campus, Fortaleza, Ceará 60455-760, Brazil

[g]Physics Department, Faculty of Science, Tanta University, Al-Geish st., Tanta 31527, Egypt

[h]Functional Materials and Devices Laboratory, Department of Materials Science and Engineering, University of Sheffield, S1 3JD, UK

*Corresponding Author: E-mail: zhoudi1220@gmail.com

Abstract: Low sintering temperature Bi[V$_{1-x}$(Fe$_{1/3}$W$_{2/3}$)$_x$]O$_4$ (BVFWx) (0.02 ≤ x ≤ 0.08) ceramics have been prepared by solid-state reaction. Compositions with 0.02 ≤ x ≤ 0.08 were scheelite-structure, but distortion of [BO$_4$] tetrahedra decreased with increase in

x. Although the crystal class remained monoclinic, the phase transition temperature (T_C) decreased from 255 °C (BV) to 51 °C (BVFW0.08), suggesting that higher concentrations of ($Fe_{1/3}W_{2/3}$) would result in the stabilization of tetragonal scheelite at room temperature. The decrease in the [BO_4] distortion additionally resulted in a large reduction in the magnitude of the temperature coefficient of resonant frequency (TCF) with near-zero values obtained by sintering BVFW0.08:2BVFW0.06 at 780 °C to give TCF ≈ -5.9 ppm / °C, relative permittivity ε_r ≈ 77.4, and microwave quality factor, $Q \times f$ ≈ 8,100 GHz (@ ~ 4.3 GHz). These promising microwave dielectric properties coupled with the low sintering temperature suggest that BVFWx ceramics are of interest in low-temperature cofired ceramic (LTCC) technology, and for monolithic resonator and filter applications.

Keywords: $BiVO_4$, microwave dielectric ceramics, low sintering temperature

1. Introduction

Low-temperature cofiring ceramic (LTCC) technology is an important method to miniaturize and multifunalize electronic components [1, 2]. It is commonly used for microwave substrate applications which are manufactured from low permittivity (ε_r) microwave dielectric ceramics. In contrast, resonators, filters and capacitors often require higher ε_r. Irrespective of the proposed application, the essential requirements for MW ceramics, remain low dielectric loss or high quaity factor (Q = 1/tanδ), a near zero temperature coefficient of resonant frequency (TCF), and in the case of LTCC, a low sintering temperature (< 950 °C) [3]. The majority of ceramic systems have obvious deficiencies with respect to MW applications, such as high sintering temperature (> 950 °C) which prohibits their use as LTCC substrates and/or large TCF. A near-zero TCF is critical in electronic devices as it permits normal operation within a wide temperature range (-25 to +85 °C).

To reduce the sintering temperature of microwave dielectric ceramics, many methods have been attempted such as the use of nano-powders [4], chemical synthesis [5] and the addition of a low melting point glass or ceramic compounds [3, 6, 7]. Several material types with promising dielectric properties however, have an intrinsically low

melting point, such as phosphates [8], borates [9], molybdates [10], vanadates [11, 12], tellurates [13] and some silicates [14]. These materials are often explored in the development LTCC technology and $BiVO_4$ is one such compound.

BiVO$_4$ has four crystal structures: orthorhombic (pucherite); scheelite monoclinic (clinobisvanite); zircon (dreyerite) and scheelite tetragonal [15-18]. In particular, monoclinic scheelite $BiVO_4$ has been widely researched for applications in antennas, filters and resonators due to its low melting temperature (820 °C) and promising micowave dielectric properties (ε_r ~ 68, TCF ~ -260 ppm/°C and $Q \times f$ ~ 6,800) [19, 20]. Unfortunately, $BiVO_4$ reacts with Ag [19] at the sintering temperature and has a large -ve TCF, both of which preclude its use in LTCC technology [20, 21]. Attempts to improve the microwave dielectric properties of $BiVO_4$ have mainly focused on the formation of solid solutions or mixtures with other end members. Lanthanides (including Y^{3+}) have a similar ionic radius to Bi^{3+} (1.17 Å) [22] and are promising substituents in $BiVO_4$ ceramics. $(Bi_{1-x}M_x)VO_4$ (M = Ce, Y) were reported to consist of monoclinic scheelite and a tetragonal zircon phase with optimum compositions giving ε_r ~ 45, TCF ~ +12 ppm/°C and $Q \times f$ ~15,000 GHz. The variation in TCF conformed to a simple mixing rule as the concentration of the lower dielectric constant zircon phase increased [23].

Despite having a dissimilar ionic radius to Bi^{3+}, the effect of Fe^{3+} substituted for Bi^{3+} in $BiVO_4$ has also been investigated [24]. ε_r decreases almost linearly owing to the lower ionic polarizability of Fe^{3+} with respect to Bi^{3+} (Fe^{3+} = 2.29 Å^3 < 6.12 Å^3 = Bi^{3+}) [22] and $Q \times f$ reaches a maximum value (15,000 GHz) at x = 0.08, but TCF remains -ve. Recent studies have suggested that B and $(Fe_{1/3}Mo_{2/3})^{5+}$ substitution for V^{5+} may also be effective, with the latter achieving ε_r ~ 74.8, TCF ~ +20 ppm/°C and $Q \times f$ ~ 11,500 GHz within ceramic-ceramic composites [25]. $[(Li_{0.5}Bi_{0.5})_{0.098}Bi_{0.902}][Mo_{0.098}V_{0.902}]O_4$ also densifies at low temperature (650 °C) and is chemically compatible with Al and Cu electrodes, demonstrating that stoichiometric A and B site complex substitutions may also tune the properties of $BiVO_4$-based ceramics [26]. $(1-x)BiVO_4-xCaTiO_3$ (wt%) composites have also realised promising MW properties and the large +ve TCF of $CaTiO_3$ facilitates a reduction in magnitude

of the temperature coefficient to 2.7 ppm/°C at x = 0.16 [27]. Fig. 1 summarizes various modifications of $BiVO_4$-compounds which have led to improved MW properties.
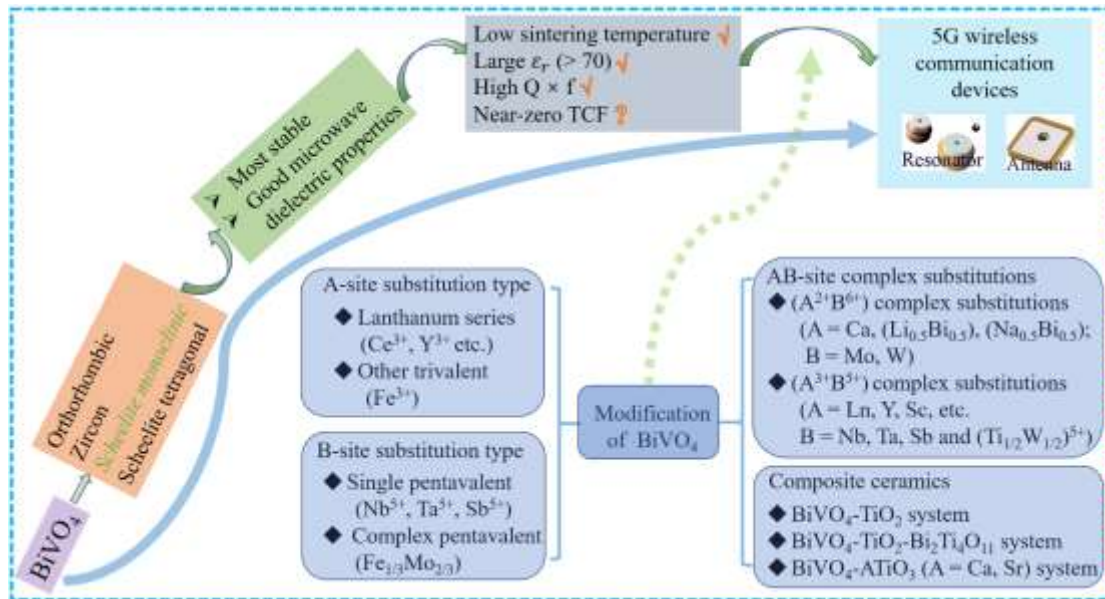
Fig. 1 Recent modification of microwave dielectric ceramics of $BiVO_4$[16, 27-32].

5 G (2-6 GHz) and future 6 G (~ 30 GHz) components require comparatively low ε_r to reduce signal delay whereas filters and resonators have traditionally utilised high ε_r materials to maximise volumetric efficiency, particularly in hand held devices where space is at a premium. A preliminary assessement suggests that the medium to large ε_r of $BiVO_4$-based materials may be most effective in capacitor or resonator applications but the ability to integate higher ε_r materials in LTCC technology is also important [33-35]. Irrespective of potential applications, the dielectric properties of $Bi[V_{1-x}(Fe_{1/3}W_{2/3})_x]O_4$ (BVFWx) ($0.02 \leq x \leq 0.08$) have been optimised in this study and the phase evolution and microstructure investigated as a function of composition and temperature.

2. Results and discussions

2.1. Phase composition and microstructure

Fig. 2 shows the XRD patterns and crystal structures of BVFWx ceramics calcined at 800 °C. As displayed in Fig. 2(a), all patterns are indexed as monoclinic scheelite but the structure exhibits a decrease in β angle for $0.02 \leq x \leq 0.08$, evidenced by the merging of (200) (020), (121) (-121), (213) (-123) and (204) (024) diffraction peaks. The

reduction in monoclinic angle is driven by a decrease in distortion of [BO$_4$] tetrahedra with increase in $(Fe_{1/3}W_{2/3})^{5+}$ concentration, similar to $(Li_{0.5x}Bi_{1-0.5x})(Mo_xV_{1-x})O_4$ and $Bi[V_{1-x}(Fe_{1/3}Mo_{2/3})_x]O_4$ systems in which the monoclinic phase is retained at room temperature up to x ~ 0.1 [25, 36]. According to several studies, four phase fields are observed as a function of composition in $BiVO_4$ compounds, as exemplified by $Bi[V_{1-x}(Fe_{1/3}Mo_{2/3})_x]O_4$: monoclinic (0 ≤ x ≤ 0.1), tetragonal (0.1 ≤ x ≤ 0.6), a composite of monoclinic $Bi(Fe_{1/3}Mo_{2/3})O_4$- and tetragonal $BiVO_4$-rich phases (0.7 ≤ x ≤ 0.9), and a $Bi(Fe_{1/3}Mo_{2/3})O_4$-rich monoclinic solid solution (0.9 ≤ x ≤ 1.0) [25]. Based on the narrow range of x investigated in this study, BVFWx appears to follow similar trends. The changes in crystal structure are also accompanied by an offset of the (112) towards smaller angles of 2θ ≈ 28.96 due to incorporation of ions with larger average radius $(R_{(Fe1/3W2/3)}^{5+} \approx 0.59$ Å, $R_V^{5+} \approx 0.54$ Å) [37] (Inset in Fig. 2a).
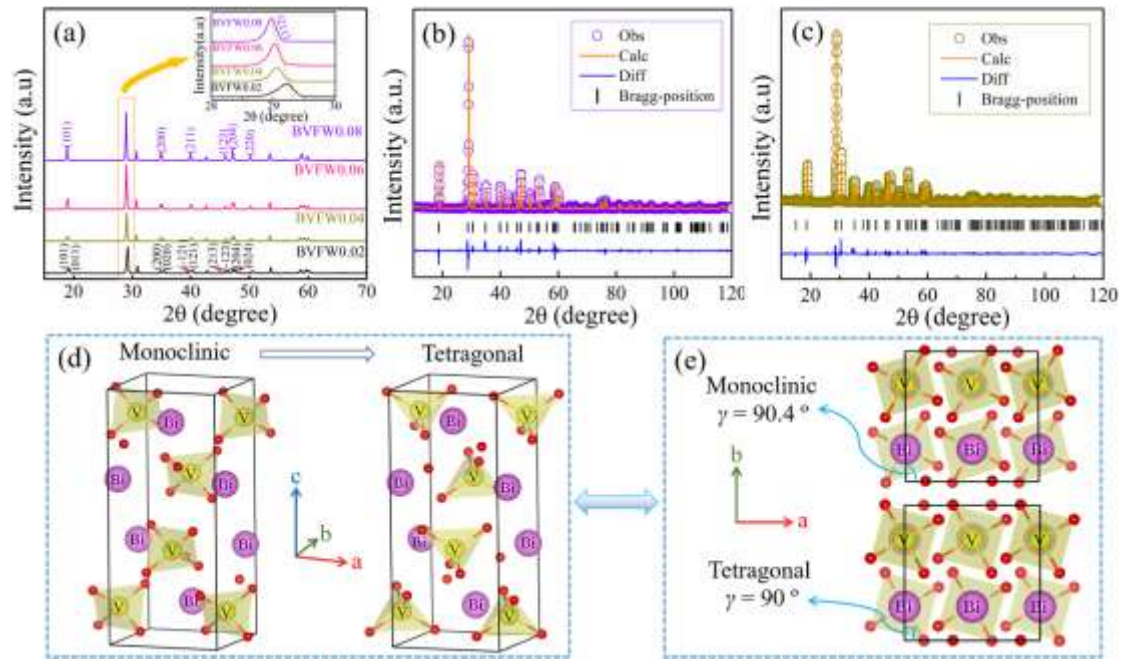
Fig. 2 (a) X-ray diffraction patterns of BVFWx (0.02 ≤ x ≤ 0.08) ceramics sintered at 800 °C. (b, c) Rietveld refinement plot of BVFW0.02 and BVFW0.08 ceramics. (d-e) Schematic diagram of crystal structure of monoclinic and tetragonal Scheelite phases.

Rietveld refinements of BVFW0.02 and BVFW0.08 are displayed in Fig. 2(b, c) with crystallographic structural parameters provided in Table S1and S2. Despite all ceramics exhibiting a monoclinic structure, the Bi-O bond lengths (Table S2) increase with x. However, the V-O$_1$ and V-O$_2$ bond lengths decrease from 1.6190 Å and 1.5677

Å to 1.5780 Å and 1.5621 Å, respectively, illustrating that the distortion of [BiO$_8$] and [VO$_4$] polyhedra reduces, without transforming to tetragonal, within the range of x investigated. The bond length of [BO$_4$] is determined by the B-site average ionic radius, which regulates the phase transformation within ABO$_4$-type scheelites. Monoclinic and tetragonal scheelite are composed of [BO$_4$] tetrahedra and [AO$_8$] dodecahedra (Fig. 2d). As illustrated, the difference between monoclinic and tetragonal relate to how the bond length of [BO$_4$] modulates the monoclinic angle which becomes effectively 0 in the tetragonal phase. The B-O bond lengths in monoclinic are unequal (B-O$_1$ > B-O$_2$) with γ = 90.4°. In contrast, in tetragonal scheelite, they are equal to give γ = 90° (Fig. 2e).
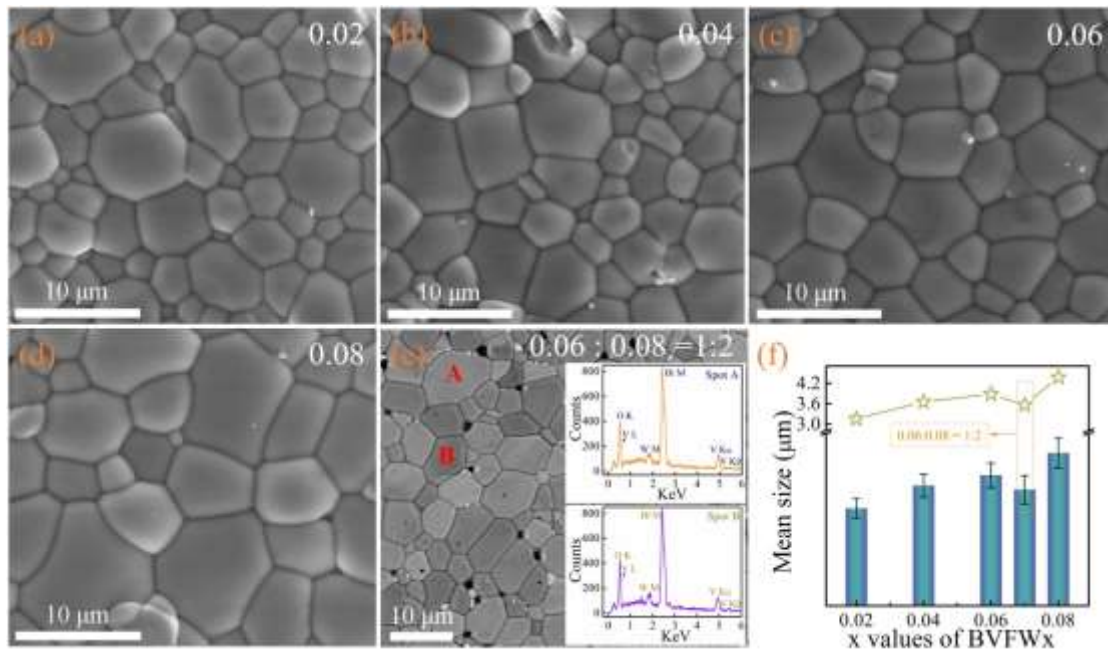
Fig. 3 (a-d) SEM images of as-fired surface of the BVFWx (0.02 ≤ x ≤ 0.08) ceramics sintered at 800 °C. (e) Backscattered scanning electron images (BSEI) and EDS of thermally etched surface of the mixture sample ($BVFW0.06 : BVFW0.08 = 1 : 2$) sintered at 780 °C. (f) Mean grain size of BVFWx ceramics as a function of x.

SEM images of the microstructure of BVFWx (0.02 ≤ x ≤ 0.08) ceramics sintered at 800 °C are shown in Fig. 3. Dense and uniform microstructures with almost no pores and well-defined grain boundaries were observed in all BVFWx compositions (Fig. 3a-d). The BSEI of the mixture, $BVFW0.06 : 2BVFW0.0$, contained a small number of pores (Fig. 3e), and grains with two distinctly different contrasts, labelled A and B. Energy Dispersive Spectroscopy (EDS) was used to obtain qualitative compositional analysis and indicated that the A and B grains had broadly similar spectra. Given the

similar composition of the two mixtures (x = 0.06 and 0.08) this is unsurprising but nonetheless, the contrast in the BSEI appears sensitive even to slight changes in chemistry. Electron tunnelling is dismissed as this would occur in all samples equally and there is no evidence of such contrast in pellets prepared as single phase rather than as a composite. In addition, there are some bright spots of secondary phases, but too little to analyze qualitatively with XRD as well as EDS. The mean grain size increases from 3.15 to 4.37 μm with x but the composite sample, Fig. 3f, has a smaller gran size which is attributed to the lower sintering temperature (780 ℃).

2.2. Raman spectra and dielectric properties
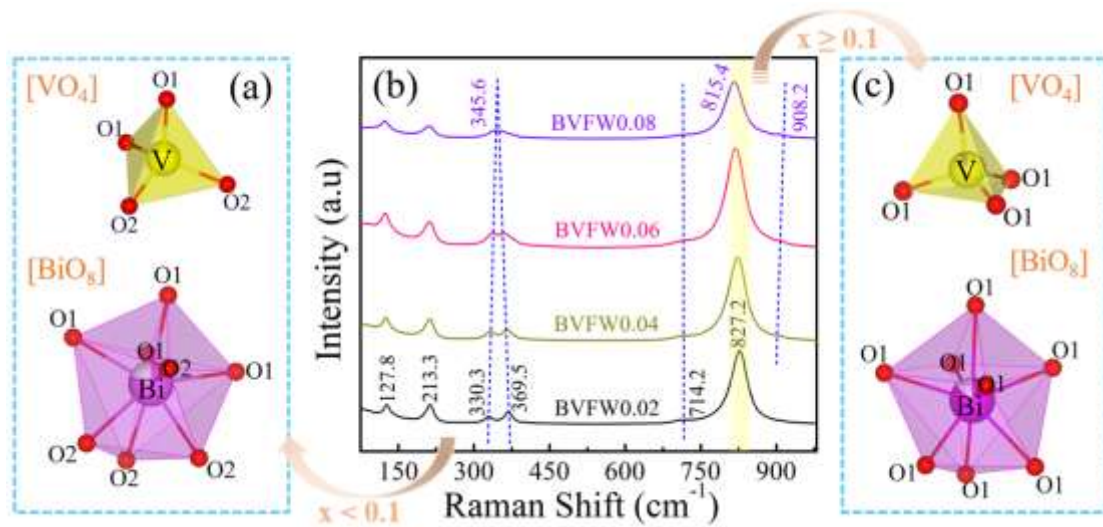
Fig. 4 Raman spectra for BVFWx (0.02 ≤ x ≤ 0.08) ceramics of (b). Schematic diagram of BiO_8 polyhedra in monoclinic (a) and tetragonal scheelite (c).

To better understand the effect of substitution of $(Fe_{1/3}W_{2/3})^{5+}$ for V^{5+} at the B-site on the phonon modes, Raman spectroscopy was conducted. Group theory predicts 9 different Raman vibrational $(3A_g + 6B_g)$ modes for monoclinic scheelite, $BiVO_4$. As shown in Fig. 4b, Raman modes around 127.8, 213.3, 330.3, 369.5, 714.2 and 827.2 cm^{-1} were observed in all samples, which are typical vibration bands of $BiVO_4$ [38]. The 127.8 and 213.3 cm^{-1} are the external modes, providing little structural information. The asymmetric and symmetric bending modes of the V-O bonds are 330.3 and 369.5 cm^{-1}, respectively. The bands at 714.2 and 827.2 cm^{-1} relate to the stretching modes of two different types of V-O bonds, and the weak shoulder at 714.2 cm^{-1} corresponds to longer V-O bonds. The strongest Raman band around 827.2 cm^{-1} is assigned to shorter

V-O bonds. The spectra and interpretation of the Raman modes are consistent with the previous studies [38-41].

The position of Raman modes is generally considered to relate to the symmetry of the crystal and its structure, whereas their width is sensitive to the 'degree of crystallinity' and is affected by point defects, and short range order on sites occupied by multiple cations [36, 40]. The strongest Raman mode at 827.2 cm^{-1} shifts to the lower wavenumber 815.4 cm^{-1} with increasing x, indicating the average bond lengths of the [VO$_4$] tetrahedra decrease and become more regular. This shift is contiguous with broadening of the mode (~ 827.2 cm^{-1}) as the distribution of ion type and size in the tetrahedra increases with x. In addition, the anti-symmetric and the symmetric bending modes at 330.3 cm^{-1} and 369.5 cm^{-1} (BVFW0.02) undergo red and blue shift, respectively. Based on the previous studies [25], the anti-symmetric and the symmetric bending modes would be expected to merge to one mode around 345.6 cm^{-1} at x = 0.1, associated with tetragonal symmetry. A schematic diagram of polyhedra in monoclinic and tetragonal scheelite BiVO$_4$ are shown in Fig. 4(a, c). For completeness, we note the characteristic vibrations of WO$_4$ groups are evidenced by υ_1 = 930 cm^{-1}, υ_2 = 838 cm^{-1} and υ_3 = 325 cm^{-1} [39] and, the Raman band at 908.2 cm^{-1} is attributed to the symmetric stretching vibration mode of W-O bond.

The measured and calculated infrared reflectance spectra of BFWVx (0.02 ≤ x ≤ 0.08) ceramics are displayed in Fig. 5. The calculations are generally expressed by Eq. (1 and 2):

$$R(\omega) = \left| \frac{1 - \sqrt{\varepsilon * (\omega)}}{1 + \sqrt{\varepsilon * (\omega)}} \right|^2 \tag{1}$$

$$\varepsilon^*(\omega) - \varepsilon(\infty) = \sum_{j=1}^{n} \frac{\omega_{pj}^2}{\omega_{oj}^2 - \omega^2 - j\gamma_j\omega} \tag{2}$$

where n is the number of polar-phonon modes, ω_{pj}, ω_{oj}, γ_j are the plasma frequency, the transverse frequency, and the linewidth (scattering rate) of the j-th Lorentz oscillator, respectively, $\varepsilon^*(\omega)$ is a complex dielectric function and ε_∞ is dielectric constant that stems from all oscillators at optical frequencies. Fig. 5a shows that some bands below
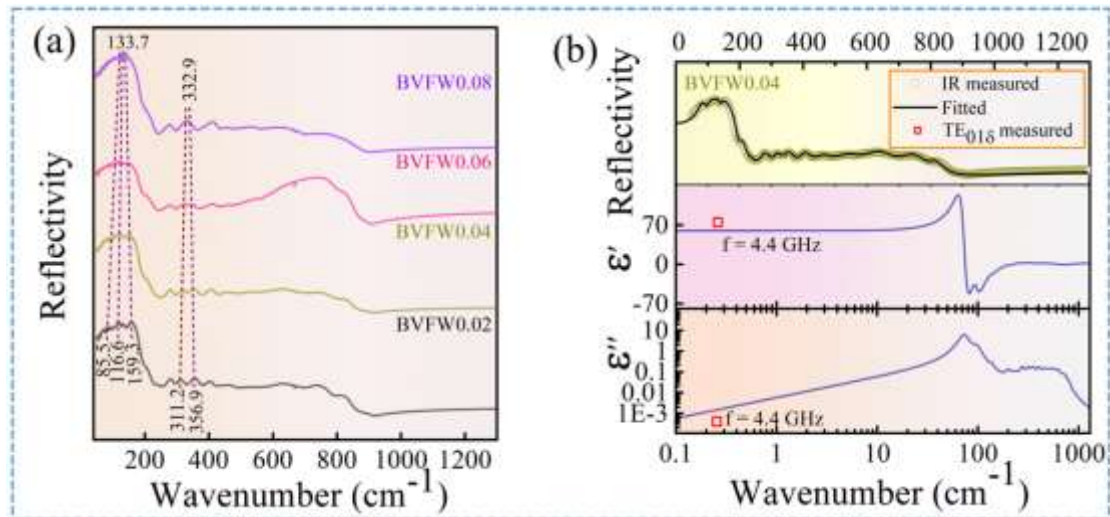
Fig. 5 (a) Experimental infrared reflection spectrum of BVFWx ($0.02 \leq x \leq 0.08$) ceramics. (b) The complex dielectric spectrum of BVFW0.04 ceramic (solid line, circle and square are fitted, experimental and measured values in microwave band).

400 cm^{-1} merge as x increases, such as the bending vibration modes at 311.2 (anti-symmetric) and 365.9 (symmetric) which converged to 332.9, indicating the potential onset of a ferroelastic phase transition from monoclinic to tetragonal scheelite at higher values x. Fig. 5b displays the experimental values of BFWV0.04 measured in the MW frequency range. The measurement and fitted spectra correspond well, confirming that the dielectric polarization is dominated by phonon absorption in the far-infrared region. The relevant phonon parameters are shown in Table S3. The external modes assigned to the Bi-O bond contributed most to ε_r, broadly in agreement with Shannon's summation rule for polarizability (Bi^{3+} = 6.12 Å^3 and V^{5+} = 2.92 Å^3, Fe^{3+} = 2.29 Å^3) but with the caveat that the polarizability of W^{6+} remains unknown as discussed in more detail in the following section. The tetrahedral bending vibration mode does not therefore, directly contribute to ε_r but the change in symmetry it induces within the cell as a whole, is still likely to influence the value of TCF.

Fig. 6 shows the permittivity, quality factor and bulk density of BVFWx ($0.02 \leq x \leq 0.08$) samples as a function of sintering temperature. ε_r, $Q \times f$ and density follow the same trend with increasing temperature, attaining a maximum at 800 °C before decreasing. According to Lichtenecker's law, a higher bulk density implies a higher relative density or lower porosity. Hence, both the optimal values of ε_r and the $Q \times f$

occur at the maximum density. In contrast for the composite mixture, $BVFW0.06:2BVFW0.08$, the optimum density and microwave dielectric properties appear at 780 ℃.
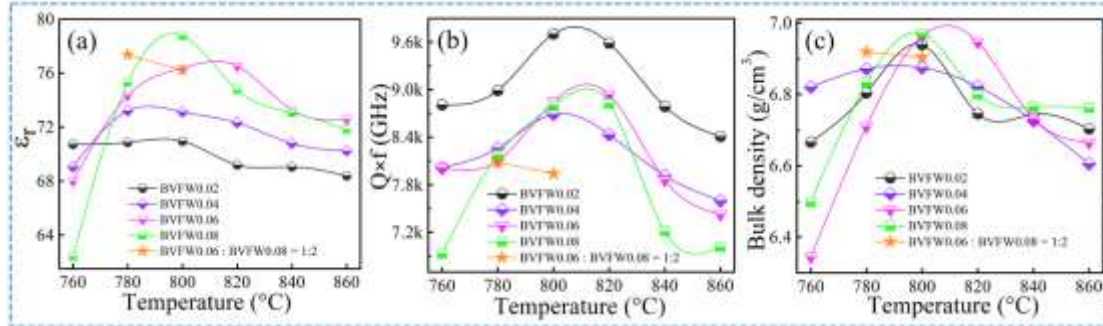
Fig. 6 The permittivity (ε_r) of (a), $Q \times f$ of (b) and bulk density of (c) for the BVFWx (0.02 ≤ x ≤ 0.08) ceramics as a function of sintering temperature.
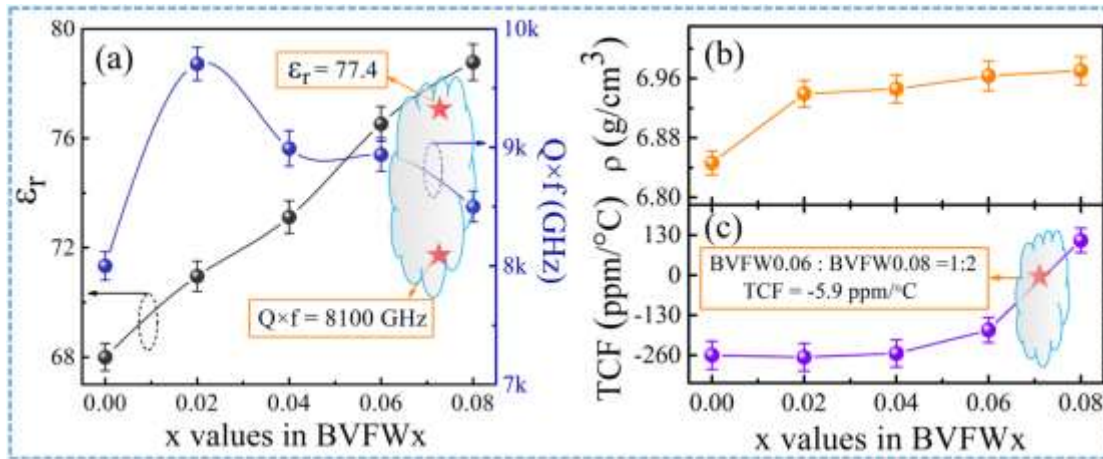
Fig. 7 (a) Permittivity (ε_r) and $Q \times f$, (b) bulk density and (c) TCF values of the BVFWx (0.02 ≤ x ≤ 0.08) ceramics as the functions of x (The red asterisk is the mixed sample of $BVFW0.06:BVFW0.08 = 1:2$).

Fig. 7 shows the microwave dielectric properties and densities of BFWVx ceramics as a function of x. As x increases, ε_r increases linearly from 68.02 to 78.78 (Fig. 7a). ε_r of ceramic materials is determined by intrinsic parameters including structural characteristics and polarizability, and extrinsic parameters such as second phase and porosity. The effect of porosity and second phase is presumed negligible based on XRD, Raman SEM and density (Fig. 7b). W^{6+} is not reported by Shannon and no direct reference to polarizability could be obtained from other literature sources. Hence, there is no strong basis to explain changes in ε_r through consideration of changes in polarizability as they are effectively unknown. We note that the gradual lowering of T_C and the decrease in V-O bond length as a function of x is commensurate

with an increase in ε_r and hence there is circumstantial evidence that crystal structure plays a role but further work is required before any conclusions can be drawn.

$Q \times f$ value increases from 8,000 GHz (4.7 GHz) to a maximum of 9,700 GHz (4.7 GHz) at BVFW0.02 and then decreases with further increase of x (Fig. 7a). The TCF increases from -260 to +113 ppm/°C with increase in x. A change in sign of TCF was also observed as a function of x in the $[(Li_{0.5}Bi_{0.5})_xBi_{1-x}][Mo_xV_{1-x}]O_4$ [26]. We propose therefore, that the vicinity of the T_C to room temperature and the structural changes associated with the transition from tetragonal and monoclinic phase are the primary tuning mechanisms for TCF.

In this study, temperature-stable microwave dielectric ceramic was obtained by creating a 1:2 molar ratio composite of compositions with x = 0.06 (-177.1 ppm/°C) and x =0.08 (+113.2 ppm/°C) which have -ve and +ve TCF, respectively, to give near zero (-5.9 ppm/°C, ★ in Fig. 7c). The mixture achieved outstanding dielectric properties with ε_r ~ 77.4, $Q \times f$ ~ 8,100 GHz (@ ~ 4.3 GHz), and TCF ~ -5.9 ppm/°C.

2.3. Thermal properties
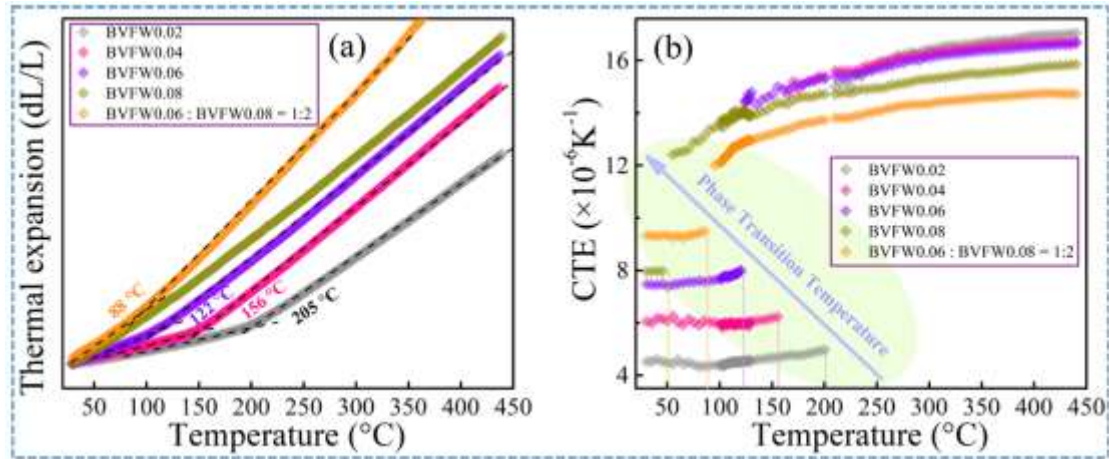
Fig. 8 The thermal properties of BVFWx (0.02 ≤ x ≤ 0.08) ceramics: (a) deformation variation, (b) coefficients of thermal expansion.

The phase transition temperature of undoped $BiVO_4$ has been reported at 255 °C [42]. To investigate accurately variations in T_C as a function of x, thermal expansion experiments were carried out (Fig. 8). The linear deformation of BVFWx increased with temperature and exhibited an inflection (T_C) at the monoclinic - tetragonal phase transition (Fig. 8a). In addition, the coefficient of thermal expansion (CTE) changes

abruptly at T_C (Fig. 8b), indicating it is larger in the tetragonal (~12 - 16) than monoclinic phase (~ 4 - 9). T_C decreases in BVFWx as a function x to 51ºC (x = 0.08), consistent with previous studies on related systems [25, 36, 43]. The decrease in T_C follows a simple mixing rule, Figure 8a, based on the general equation ($T(K) = 258(\pm 5) - 2550(\pm 50) \times x$) [25] and is directly correlated with the distortion of the B-O polyhedra.

3. Conclusions

Ceramics fabricated from $Bi[V_{1-x}(Fe_{1/3}W_{2/3})_x]O_4$ ($0.02 \leq x \leq 0.08$) scheelite solid solutions have been studied. Phase analysis was performed by XRD, with Rietveld refinements of the spectra, and Raman spectroscopy. For $0.02 \leq x \leq 0.08$, all components were monoclinic scheelite but the distortion of $[BO_4]$ tetrahedra decreased with increase in x, and the crystal structure showed evidence of progressively shifting towards but not attaining at room temperature, a stable tetragonal scheelite phase, further evidenced by the decrease in T_C from 255 °C (BV) to 51 °C (BFVW0.08). The variation of the $[BO_4]$ tetrahedral distortion and its affect on T_C influences the magnitude and sign of TCF. Optimum properties were achieved from composite mixtures of $BVFW0.06 : 2B\ VFW0.08$ with $\varepsilon_r \approx 77.4$, TCF $\approx$ -5.9 ppm / °C, and $Q \times f \approx 8,100$ GHz (@ ~ 4.3 GHz). The system is therefore, not only a candidate for use as a dielectric resonator but also in LTCC technology due to its low sintering temperature (780 ºC).

Declaration of Competing Interest

The authors declare that they have no known competing financial interests or personal relationships that could have appeared to influence the work reported in this paper.

Acknowledgments

Appendix A. Supporting information

The experimental materials, methods, and characterization of $Bi[V_{1-x}(Fe_{1/3}W_{2/3})_x]O_4$ $(0.02 \leq x \leq 0.08)$ ceramics, refined lattice parameters of $Bi[V_{1-x}(Fe_{1/3}W_{2/3})_x]O_4$ $(x = 0.02$ and $0.08)$ ceramics (Table S1 and S2), phonon parameters obtained by fitting the infrared reflection spectrum of $Bi[V_{1-x}(Fe_{1/3}W_{2/3})_x]O_4$ $(x = 0.04)$ ceramics (Table S3).

References

[1] M.T. Sebastian, H. Wang, H. Jantunen, Low temperature co-fired ceramics with ultra-low sintering temperature: A review, Curr Opin Solid State Mater Sci 20 (2016) 151-170.

[2] J. Varghese, P. Ramachandran, M. Sobocinski, T. Vahera, H. Jantunen, ULTCC glass composites based on rutile and anatase with cofiring at 400 °C for high frequency applications, ACS Sustain. Chem. Eng. 7 (2019) 4274-4283.

[3] D. Wang, L. Li, M. Du, Y. Zhan, A low-sintering temperature microwave dielectric ceramic for 5G LTCC applications with ultralow loss, Ceram. Int. 47 (2021) 28675-28684.

[4] H. Zhou, N. Wang, X. Tan, J. Huang, X. Chen, Glass-free $Li_2ZnTi_3O_8$ low temperature cofired ceramics by pretreating raw materials, J. Mater. Sci. Mater. Electron. 27 (2016) 11850-11855.

[5] S.A. da Silva, S.M. Zanetti, Processing of $Bi_{1.5}ZnNb_{1.5}O_7$ ceramics for LTCC applications: Comparison of synthesis and sintering methods, Ceram. Int. 35 (2009) 2755-2759.

[6] R. Deshmukh, V. Chaware, R. Ratheesh, G.J. Phatak, Synthesis and microwave dielectric properties of BBSZ-Zinc silicate based material for LTCC applications, J. Electron. Mater. 50 (2021) 1323-1330.

[7] F. Ebrahimi, A. Nemati, S. Banijamali, Fabrication and microwave dielectric characterization of cordierite/BZBS (Bi_2O_3-ZnO-B_2O_3-SiO_2) glass composites for LTCC applications, J. Alloys Compd. 882 (2021) 160722.

[8] C.C. Xia, D.H. Jiang, G.H. Chen, Y. Luo, B. Li, C.L. Yuan, C.R. Zhou, Microwave dielectric ceramic of $LiZnPO_4$ for LTCC applications, J. Mater. Sci. Mater. Electron. 28 (2017) 12026-12031.

[9] D. Szwagierczak, B. Synkiewicz-Musialska, J. Kulawik, N. Palka, Sintering, microstructure, and dielectric properties of copper borates for high frequency LTCC applications, Materials 14

(2021) 4017.

[10] P. Yadav, E. Sinha, Structural, photophysical and microwave dielectric properties of α-ZnMoO$_4$ phosphor, J. Alloys Compd. 795 (2019) 446-452.

[11] H. Zhou, F. He, X. Chen, J. Chen, L. Fang, Series of thermally stable Li$_{1+2x}$Mg$_{4-x}$V$_3$O$_{12}$ ceramics: low temperature sintering characteristic, crystal structure and microwave dielectric properties, J. Mater. Sci. Mater. Electron. 25 (2014) 1480-1484.

[12] G.G. Yao, C.J. Pei, J.G. Xu, P. Liu, J.P. Zhou, H.W. Zhang, Microwave dielectric properties of CaV$_2$O$_6$ ceramics with low dielectric loss, J. Mater. Sci. Mater. Electron. 26 (2015) 7719-7722.

[13] L. Fang, Z. Wei, H. Guo, Y. Sun, Y. Tang, C. Li, Phase composition and microwave dielectric properties of low-firing Li$_2$A$_2$W$_3$O$_{12}$ (A = Mg, Zn) ceramics, J. Mater. Sci. Mater. Electron. 26 (2015) 5892-5895.

[14] M. Valant, D. Suvorov, Glass-free low-temperature cofired ceramics: calcium germanates, silicates and tellurates, J. Eur. Ceram. Soc. 24 (2004) 1715-1719.

[15] A. Pinczuk, B. Welbe, F.H. Dacol, Mechanism of the Ferroelastic Transition of BIVO$_4$, Solid State Commun 29 (1979) 515-518.

[16] D. Zhou, L.-X. Pang, D.-W. Wang, I.M. Reaney, BiVO$_4$ based high k microwave dielectric materials: a review, J. Mater. Chem. C 6 (2018) 9290-9313.

[17] S. Tokunaga, H. Kato, A. Kudo, Selective preparation of monoclinic and tetragonal BiVO$_4$ with scheelite structure and their photocatalytic propertie, J Mater. Chem. 13 (2001) 4624-4628.

[18] P. Pookmanee, S. Kojinok, S. Phanichphant, Bismuth vanadate (BiVO$_4$) powder prepared by the sol-gel method, Journal of Metals, Materials and Minerals 22 (2012) 49-53.

[19] M. Valant, D. Suvorov, Chemical Compatibility between Silver Electrodes and Low-Firing Binary-Oxide Compounds: Conceptual Study, J. Am. Ceram. Soc. 83 (2000) 2721-2729.

[20] M.T. Sebastian, R. Ubic, H. Jantunen, Low-loss dielectric ceramic materials and their properties, Int. Mater. Rev. 60 (2015) 392-412.

[21] M.T. Sebastian, H. Jantunen, Low loss dielectric materials for LTCC applications: a review, Int. Mater. Rev. 53 (2013) 57-90.

[22] R.D. Shannon, Dielectric polarizabilities of ions in oxides and fluorides, Jpn. J. Appl. Phys. 73 (1993) 348-366.

[23] D. Zhou, W.-B. Li, H.-H. Xi, L.-X. Pang, G.-S. Pang, Phase composition, crystal structure, infrared reflectivity and microwave dielectric properties of temperature stable composite ceramics (scheelite and zircon-type) in BiVO$_4$-YVO$_4$ system, J. Mater. Chem. C 3 (2015) 2582-2588.

[24] D. Zhou, H. Bin, J. Guo, L.-X. Pang, Z.-M. Qi, T. Shao, Q.-P. Wang, Z.-X. Yue, X. Yao, C. Randall, Phase evolution and microwave dielectric properties of (Bi$_{1-x}$Fe$_x$)VO$_4$ (x$\leq$ 0.40) ceramics, J. Am. Ceram. Soc. 97 (2014) 2915-2920.

[25] D. Zhou, L.-X. Pang, J. Guo, Z.-M. Qi, T. Shao, X. Yao, C.A. Randall, Phase evolution, phase transition, and microwave dielectric properties of scheelite structured xBi(Fe$_{1/3}$Mo$_{2/3}$)O$_4$-(1-x)BiVO$_4$ (0.0 ≤ x ≤ 1.0) low temperature firing ceramics, J. Mater. Chem. 22 (2012) 21412.

[26] D. Zhou, C.A. Randall, H. Wang, L.-X. Pang, X. Yao, Ultra-low firing high-k scheelite structures based on $[(Li_{0.5}Bi_{0.5})_xBi_{1-x}][Mo_xV_{1-x}]O_4$ microwave dielectric ceramics, J. Am. Ceram. Soc. 93 (2010) 2147-2150.

[27] R.G.M. Oliveira, R.A. Silva, J.E.V. de Morais, G.S. Batista, M.A.S. Silva, J.C. Goes, H.D. de Andrade, I.S. Queiroz Júnior, C. Singh, A.S.B. Sombra, Effects of $CaTiO_3$ addition on the microwave dielectric properties and antenna properties of $BiVO_4$ ceramics, Compos. B. Eng. 175 (2019) 107122.

[28] P.V. Bijumon, S. Solomon, M.T. Sebastian, A new group of microwave dielectric ceramics in the $RE(Ti_{0.5}W_{0.5})O_4$ [RE = Pr, Nd, Sm, Gd, Tb, Dy, and Y] system, J. Mater. Sci.-Mater. El. 14 (2003) 5-8.

[29] G.H. Chen, F.F. Gu, M. Pan, L.Q. Yao, M. Li, X. Chen, Y. Yang, T. Yang, C.L. Yuan, C.R. Zhou, Microwave dielectric properties of $BiVO_4/Li_{0.5}Re_{0.5}WO_4$ (Re = La, Nd) ultra-low firing ceramics, J. Mater. Sci.-Mater. El. 26 (2015) 6511-6517.

[30] F.-F. Gu, G.-H. Chen, X.-L. Kang, X. Li, C.-R. Zhou, C.-L. Yuan, Y. Yang, T. Yang, A new $BiVO_4/Li_{0.5}Sm_{0.5}WO_4$ ultra-low firing high-k microwave dielectric ceramic, J. Mater. Sci. 50 (2014) 1295-1299.

[31] Z. Wang, C. Yuan, Q. Li, Q. Feng, F. Liu, Y. Yang, C. Zhou, G. Chen, Microwave dielectric properties of $(1-x)BiVO_4-xLn_{2/3}MoO_4$ (Ln=Er, Sm, Nd, la) ceramics with low sintering temperatures, J. Electroceram. 40 (2017) 99-106.

[32] R.G.M. Oliveira, J.E.V. de Morais, G.S. Batista, M.A.S. Silva, J.C. Goes, A.S.B. Sombra, Dielectric characterization of $BiVO_4-TiO_2$ composites and applications in microwave range, J. Alloys Compd. 775 (2019) 889-895.

[33] H. Jantunen, T. Kangasvieri, J. Vähäkangas, S. Leppävuori, Design aspects of microwave components with LTCC technique, J. Eur. Ceram. Soc. 23 (2003) 2541-2548.

[34] R.A.U. Rahman, D.E.J. Ruth, M. Ramaswamy, Emerging scenario on displacive cubic bismuth pyrochlores $(Bi,M)MNO_{7-\delta}$ (M = transition metal, N = Nb, Ta, Sb) in context of their fascinating structural, dielectric and magnetic properties, Ceram. Int. 46 (2020) 14346-14360.

[35] M. Valant, G.S. Babu, M. Vrcon, T. Kolodiazhnyi, A.-K. Axelsson, Pyrochlore range from $Bi_2O_3-Fe_2O_3-TeO_3$ system for LTCC and photocatalysis and the crystal structure of new $Bi_3(Fe_{0.56}Te_{0.44})_3O_{11}$, J. Am. Ceram. Soc. 95 (2012) 644-650.

[36] D. Zhou, W.G. Qu, C.A. Randall, L.X. Pang, H. Wang, X.G. Wu, J. Guo, G.Q. Zhang, L. Shui, Q.P. Wang, H.C. Liu, X. Yao, Ferroelastic phase transition compositional dependence for solid-solution $[(Li_{0.5}Bi_{0.5})_xBi_{1-x}][Mo_xV_{1-x}]O_4$ scheelite-structured microwave dielectric ceramics, Acta Mater. 59 (2011) 1502-1509.

[37] R.D. Shannon, Revised effective ionic radii and systematic studies of interatomie distances in halides and chaleogenides, Acta Crystallogr. A32 (1976) 751-767.

[38] R.L. Frost, D.A. Henry, M.L. Weier, W. Martens, Raman spectroscopy of three polymorphs of $BiVO_4$: clinobisvanite, dreyerite and pucherite, with comparisons to $(VO_4)_3$-bearing minerals: namibite, pottsite and schumacherite, J Raman Spectrosc 37 (2006) 722-732.

[39] N. Weinstock, H. Schulze, A. Müller, Assignment of ν2(E) and ν4(F2) of tetrahedral species by the calculation of the relative raman intensities: The vibrational spectra of VO43-, CrO42-, MoO42-, WO42-, MnO4-, TcO4-, ReO4-, RuO4, and OsO4, J. Chem. Phys. 59 (1973) 5063-5067.

[40] H.M. Zhang, J.B. Liu, H. Wang, W.X. Zhang, H. Yan, Rapid microwave-assisted synthesis of phase controlled $BiVO_4$ nanocrystals and research on photocatalytic properties under visible light irradiation, J Nanopart Res 10 (2007) 767-774.

[41] Y.K. Kshetri, B. Chaudhary, T. Kamiyama, T.-H. Kim, F. Rosei, S.W. Lee, Determination of ferroelastic phase transition temperature in $BiVO_4$ by raman spectroscopy, Mater. Lett. 291 (2021) 129519.

[42] R.M. Hazen, J.W.E. Mariathasan, Bismuth vanadate: a high-pressure, high-temperature crystallographic study of the ferroelastic-paraelastic transition., Science 216 (1982) 991.

[43] D. Zhou, L.X. Pang, J. Guo, H. Wang, X. Yao, C. Randall, Phase evolution, phase transition, raman spectra, infrared spectra, and microwave dielectric properties of low temperature firing $(K_{0.5x}Bi_{1-0.5x})(Mo_xV_{1-x})O_4$ ceramics with scheelite related structure, Inorg. Chem. 50 (2011) 12733-12738.

ToC Figure: